

# 1 Criticality of plasma membrane 2 lipids reflects activation state of 3 macrophage cells

4 Eugenia Cammarota<sup>\*1,2</sup>, Chiara Soriani<sup>1</sup>, Raphaëlle Taub<sup>1</sup>, Fiona Morgan<sup>1</sup>, Jiro  
5 Sakai<sup>3</sup>, Sarah L. Veatch<sup>4</sup>, Clare E. Bryant<sup>3</sup>, Pietro Cicuta<sup>\*1</sup>

**\*For correspondence:**

[eu.cammarota@gmail.com](mailto:eu.cammarota@gmail.com) (EC);  
[pc245@cam.ac.uk](mailto:pc245@cam.ac.uk) (PC)

6 <sup>1</sup>Cavendish Laboratory, University of Cambridge, Cambridge CB3 0HE, United Kingdom;  
7 <sup>2</sup>Experimental Imaging Center, San Raffaele Hospital, Milan, Italy; <sup>3</sup>Department of  
8 Veterinary Medicine, University of Cambridge, Cambridge CB3 0ES, United Kingdom ;  
9 <sup>4</sup>Biophysics Department, University of Michigan, Ann Arbor, MI 48109, USA

---

11 **Abstract** Signalling is of particular importance in immune cells, and upstream in the signalling  
12 pathway many membrane receptors are functional only as complexes, co-locating with particular  
13 lipid species. Work over the last 15 years has shown that plasma membrane lipid composition is  
14 close to a critical point of phase separation, with evidence that cells adapt their composition in  
15 ways that alter the proximity to this thermodynamical point. Macrophage cells are a key  
16 component of the innate immune system, responsive to infections, regulating the local state of  
17 inflammation. We investigate changes in the plasma membrane's proximity to the critical point, as  
18 a response to stimulation by various pro- and anti-inflammatory agents. Pro-inflammatory (IFN- $\gamma$ ,  
19 Kdo-LipidA, LPS) perturbations induce an increase in the transition temperature of the GMPVs;  
20 anti-inflammatory IL4 has the opposite effect. These changes recapitulate complex plasma  
21 membrane composition changes, and are consistent with lipid criticality playing a master  
22 regulatory role: being closer to critical conditions increases membrane protein activity.

---

## 24 Introduction

25 Macrophages are extremely versatile cells of the innate immune system able to activate and  
26 adapt their functionality depending on the specific milieu *Martinez and Gordon (2014)*. Following  
27 phagocytosis of material resulting from trauma, or pathogens, or detection of specific functional  
28 molecules, macrophages can change their gene regulatory state and polarize into activated states,  
29 where for example they produce immune effector molecules such as cytokines for intercellular  
30 communication *Taylor et al. (2005)*; *Mosser and Edwards (2008)*; *Brandsma et al. (2018)*. The  
31 responses manifested as a consequence of different stimulations have been classified in two broad  
32 activation states, based on both genetic expression profiling and phenotypic behavior: M1, or  
33 classically activated, macrophages have an enhanced bactericidal and tumoricidal capacity and  
34 produce high levels of pro-inflammatory cytokines, while M2 macrophages produce low levels of  
35 cytokines and have a wound-healing capacity by contributing to the production of collagen and  
36 extracellular matrix *Martinez and Gordon (2014)*; *Lawrence and Natoli (2011)*; *Mosser and Edwards*  
37 *(2008)*. The stimuli that promote M1 macrophage activation are mainly IFN- $\gamma$ , LPS and GM-CSF.  
38 IFN- $\gamma$  is a cytokine mainly produced by natural killer (NK) and T helper 1 (Th1) cells; signaling from  
39 the IFN- $\gamma$  receptor (IFNGR) controls the regulation of specific genes related to the production of  
40 cytokine receptors, cell activation markers and adhesion molecules *Martinez and Gordon (2014)*.

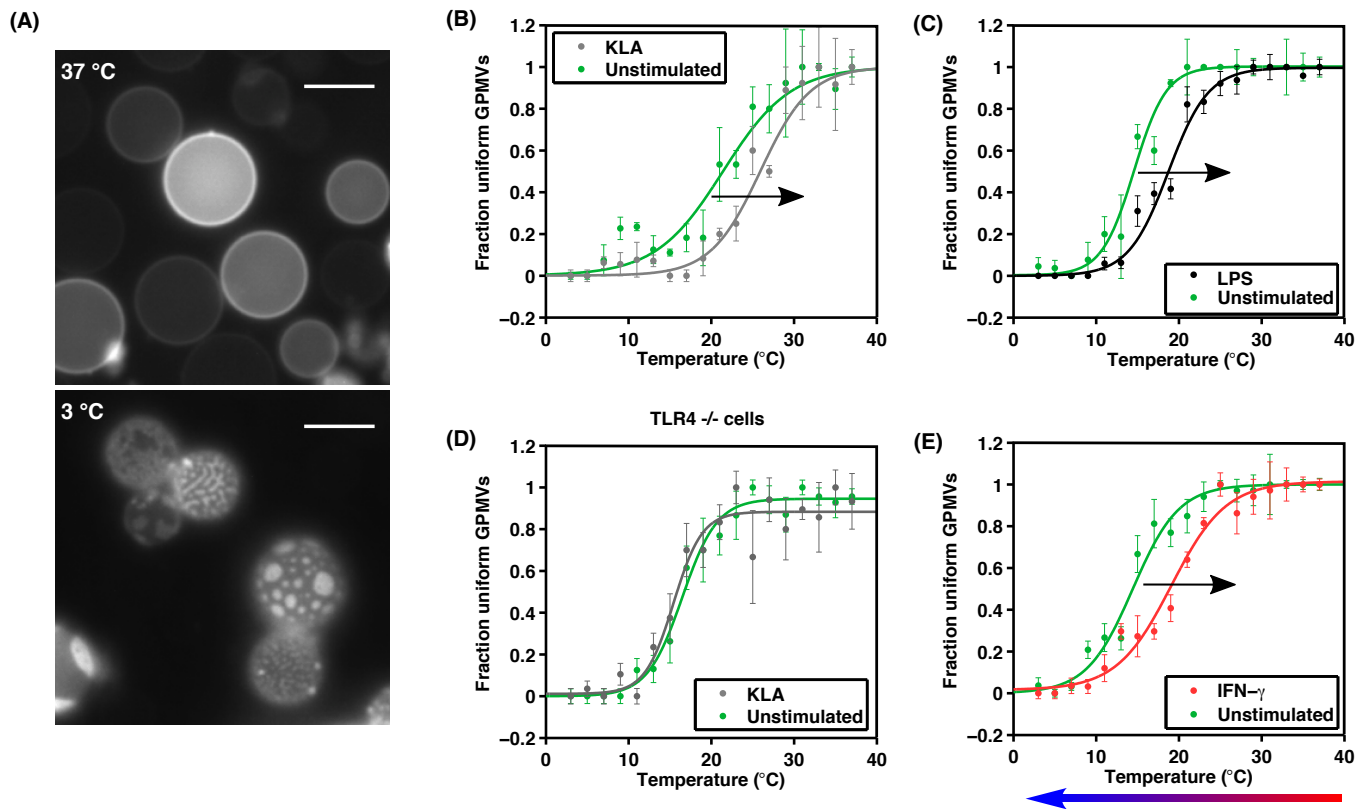


**Figure 1. The plasma membrane of macrophage cells is poised close to phase separation, and the proximity to the critical point varies in response to signaling molecules.** (A): Fluorescence microscope image of GPMVs at 37 and 3°C. Scalebar 5 $\mu$ m. (B-E): Fraction of GPMVs showing just one phase over the total of vesicles observed in function of the temperature. The data show a sigmoidal trend and are fitted with a hyperbolic tangent from which are extracted the transition temperature at mid height and the width of the transition. We compare the sample obtained from cells treated with KdoLipidA (B), LPS (C), IFN- $\gamma$  (E), for 12h compared to a non-treated control condition prepared in parallel. All these “pro-inflammatory” treatments shift the transition temperature towards higher temperatures. The colored arrow at the bottom indicates the direction of the temperature variation imposed on the GPMV samples during the imaging process. (D): The knock-out TLR4<sup>-/-</sup> cells do not vary transition temperature when stimulated with KdoLipidA (in contrast to panel (A)), remaining the same to the unstimulated controls.

41 Lipopolysaccharides (LPS) are a class of molecules of the outer membrane of gram-negative bacteria,  
 42 these molecules are recognized by the TLR4 receptor *Park et al. (2009); Kawai and Akira (2010)*.  
 43 TLR4 activation triggers the downstream production of pro-inflammatory cytokines such as TNF- $\alpha$   
 44 and presentation of antigens *Akira and Takeda (2004)*. In contrast, macrophages polarize into M2  
 45 mainly in response to IL4 and IL13 stimuli. IL4 is produced by T helper 2 (Th2) cells, basophils, and  
 46 mast cells in response to a tissue injury and in presence of some fungi and parasites *Mosser and*  
 47 *Edwards (2008)*. M2 cells are sensitive to infections, their production of pro-inflammatory cytokines  
 48 is minimal, and their phagocytic activity is low *Martinez and Gordon (2014); Mosser and Edwards*  
 49 *(2008)*.

50 In the transduction of signals a fundamental regulatory role is thought to be played by the  
 51 plasma membrane composition *Simons and Toomre (2000)*. There are many examples of specific  
 52 protein-lipid affinity, but also strong evidence of more general mechanisms such as the propensity  
 53 of lipid mixtures to form cholesterol rich domains, or domains of a preferred thickness, which  
 54 then imply a preferred partitioning of certain transmembrane proteins *Simons and Sampaio (2011);*  
 55 *Stone et al. (2017); Veatch and Cicuta (2018)*. Any mechanism that modifies local recruitment of  
 56 membrane proteins, in the context of an assembly step such as dimerization necessary for function,  
 57 can therefore directly be a regulator of receptor activity. This generalises a well known theme in  
 58 membrane biochemistry, that proteins with lipid raft affinity have a higher chance to interact *Pralle*  
 59 *et al. (2000)*. The key structures in this study of macrophages, the TLR4 receptor and its co-receptor

60 CD14, are both known to have raft affinity: CD14 is found in lipid rafts both before and after LPS  
61 activation, while TLR4 receptors are initially found in non-raft regions and then translocate to rafts  
62 after the activation *Triantafilou et al. (2002)*. It has also been shown that the use of lipid raft  
63 inhibitors reduces significantly the production of cytokines related to LPS activation *Nakahira et al.*  
64 *(2006)*. Moreover, lauric fatty acid seems to be responsible for the recruitment and dimerization of  
65 TLR4 into lipid rafts *Wong et al. (2009)*. All together these facts strongly hint that plasma membrane  
66 composition, and in particular the propensity to form lipid rafts or domains, are fundamental  
67 regulators of protein interaction; we explore this theme with respect to activation of macrophages  
68 and the activity of TLR4 receptors.

69 Various authors have put forward the idea that the lipid raft phenomenology is linked to the  
70 propensity for the lipidic component of the membrane to undergo liquid-liquid separation *Veatch*  
71 *and Cicuta (2018)*, as was observed in plasma membrane extracts *Veatch et al. (2008)*. Vesicles  
72 extracted from the plasma membrane of cells have the same characteristics of certain ternary lipid  
73 mixtures, of particular interest the spontaneous appearance of transient lipid domains which is a  
74 universal property of systems in vicinity of a critical point *Veatch et al. (2008)*; *Honerkamp-Smith*  
75 *et al. (2008)*. From a biological point of view, being poised close to a critical point could be advan-  
76 tageous to accelerate a whole set of membrane biochemistry, since the cell would require much  
77 less energy to create lipid heterogeneity. Modulating the lipid composition is thus a mechanism for  
78 global regulation of activity on the membrane *Veatch and Cicuta (2018)*. Giant plasma membrane  
79 vesicles (GPMVs) allow to study the properties of the membrane lipids as isolated systems *Scott*  
80 *(1976)*; *Scott and Maercklein (1979)*. These vesicles are thought to maintain the protein and lipid  
81 diversity of the mother membrane *Scott and Maercklein (1979)*; *Fridriksson et al. (1999)*, and at  
82 low temperatures the lipids can phase separate laterally into micron sized domains *Baumgart et al.*  
83 *(2007)*; *Veatch et al. (2008)*; *Kaiser et al. (2009)*. GPMVs as systems to study the criticality of the  
84 plasma membrane have shown systematic dependency on growth temperature *Gray et al. (2015)*  
85 and cell cycle *Burns et al. (2017)*, and on the epithelial-mesenchymal transition in cancer cells *Tisza*  
86 *et al. (2016)*, and indeed in both situations the transition temperature of GPMVs recapitulates broad  
87 systematic composition changes that move the cell composition closer or farther from the critical  
88 point. In literature there are previous studies on the effect on lipid composition of macrophage  
89 activation *Dennis et al. (2010)*; *Andreyev et al. (2010)*, but these are bulk assays and report on the  
90 changes in a huge number of lipid species, making it difficult to interpret the results in simple  
91 terms. The work presented here shows that these complex changes in lipidomics may have a  
92 simple interpretation, in terms of their effect on the membrane phase separation. Investigating the  
93 effects of different kinds of macrophage cell stimulants (LPS, KLA, IFN- $\gamma$ , IL4), known to differentiate  
94 macrophages into two different activation states, we show opposite changes with respect to the  
95 proximity of the critical point in the two cell types, consistent with biological function.

## 96 **Materials and methods**

### 97 **Cell Culture**

98 The immortalized BMDM cell lines were obtained from Dr. Eicke Latz (Institute of Innate Immunity  
99 at the University of Bonn, Bonn, Germany), and Dr. Kate Fitzgerald and Dr. Douglas T. Golenbock  
100 (University of Massachusetts Medical School, MA, USA). C57BL6 TLR4<sup>-/-</sup> mice were obtained from  
101 Dr. S.Akira (Osaka University, Osaka, Japan) *Hoshino et al. (1999)*. iBMDM and TLR4<sup>-/-</sup> iBMDM were  
102 maintained in Dulbecco's Modified Eagle's Medium (DMEM; Sigma-Aldrich, MO, USA) supplemented  
103 with 10% (v/v) heat-inactivated Hyclone fetal calf serum (FCS; Thermo Scientific, UT, USA), 2mM L-  
104 glutamine (Sigma-Aldrich), 100 U/mL penicillin and streptomycin (Sigma-Aldrich), and 20mM HEPES  
105 (Sigma-Aldrich). Cells are cultured for at least two days and brought to confluence in a single  
106 175 cm<sup>2</sup> flask. From confluence, cells are plated in separate dishes. To test the effect of stimulants  
107 on the melting temperature an equal number of cells are plated for each condition; we use a  
108 density of about 6-7·10<sup>3</sup> cells/mm<sup>2</sup>. After 12 hours the culture medium is changed with (or without

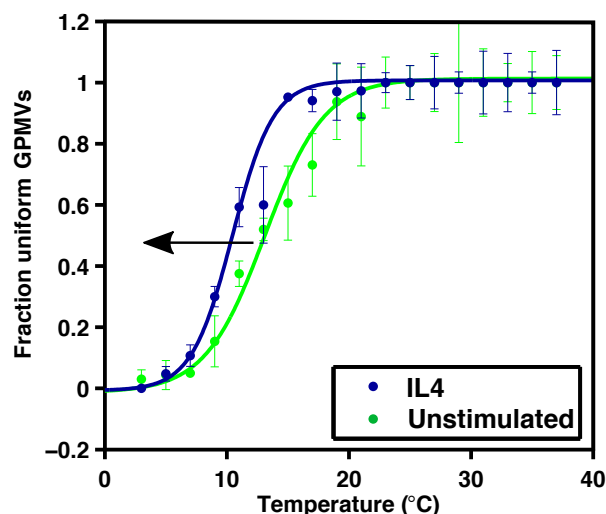


**Figure 2. Anti-inflammatory treatment moves the composition of the plasma membrane farther from the critical point.** The data show the fraction of uniform GPMVs as the temperature of the sample is varied. The two curves correspond to 24 hours of IL4 stimulation and to unstimulated conditions.  $T_{UNST} = (13.11 \pm 0.49)^{\circ}\text{C}$ ,  $T_{IL4} = (10.46 \pm 0.33)^{\circ}\text{C}$ .

109 for the control condition) the addition of stimulating agents. Then, after the stimulation time,  
110 12 hours, we start the GPMVs production protocol. Cell stimulating agents are used at the following  
111 concentrations: IFN- $\gamma$  20 ng/ml (PeproTech); LPS from *Salmonella* Typhimurium 10 ng/ml (Enzo Life  
112 Sciences); Kdo-LipidA 100 ng/ml (KLA, Avanti Polar Lipids); IL-4 20 ng/ml (PeproTech), and left for  
113 12 or 24 hours. These doses were chosen according to previous work on M1/M2 macrophage  
114 differentiation *Vats et al. (2006)*; *Tatano et al. (2014)* *Kigerl et al. (2009)*.

115 To measure the  $T_m$  vs cell density dependency, density was measured in two different ways. For  
116 some experiments, images of the culture were acquired with a low magnification objective and the  
117 density estimated by counting cells from the image and then dividing their number by the field  
118 of view area. The same dish was then used to produce GPMVs immediately after. Otherwise for  
119 each density we had twin dishes, one was used to count the cells with the hemocytometer, whilst  
120 the other was used to produce GPMVs. To check the effect of stimulation on growth rate, an equal  
121 number of cells were plated in a multi-well then, for each condition (control, IL4, LPS); cells were  
122 counted with the hemocytometer after cell adhesion (0h), then stimulated, according to previously  
123 specified concentrations, and counted after 12h. Cells were initially plated to have about  $6\text{-}7 \cdot 10^3$   
124 cells/mm<sup>2</sup> at 0h.

### 125 GPMVs production

126 The procedure for membrane labeling and GPMVs production follows the protocols in *Sezgin*  
127 *et al. (2012)* and *Gray et al. (2013)*. The cells are gently washed twice with PBS, then Dil-C12(3)  
128 (Life Technologies) dye solution 50  $\mu\text{g}/\text{ml}$  in PBS is added and left on ice for 10 minutes to allow  
129 incorporation into the membrane. Then the cells are washed five times with PBS and twice with  
130 GPMV buffer. GPMV buffer is formed by 10mM HEPES, 150mM NaCl, 2mM CaCl<sub>2</sub>, the pH is adjusted  
131 to 7.4 with HCl or NaOH. Lastly the vesiculating agent is added and the cells are left in the incubator  
132 for 1.5 hours at 37°C. 20  $\mu\text{l}$  of vesiculating agent (2mM DTT, 25mM PFA) is used for each ml of GPMV  
133 buffer. The medium is gently harvested and transferred into a falcon tube. The sample is left at  
134 37°C enough to let the blebs deposit on the bottom of the tube: for a volume of 4 ml, 24 hours are  
135 enough for the whole sample to sediment.

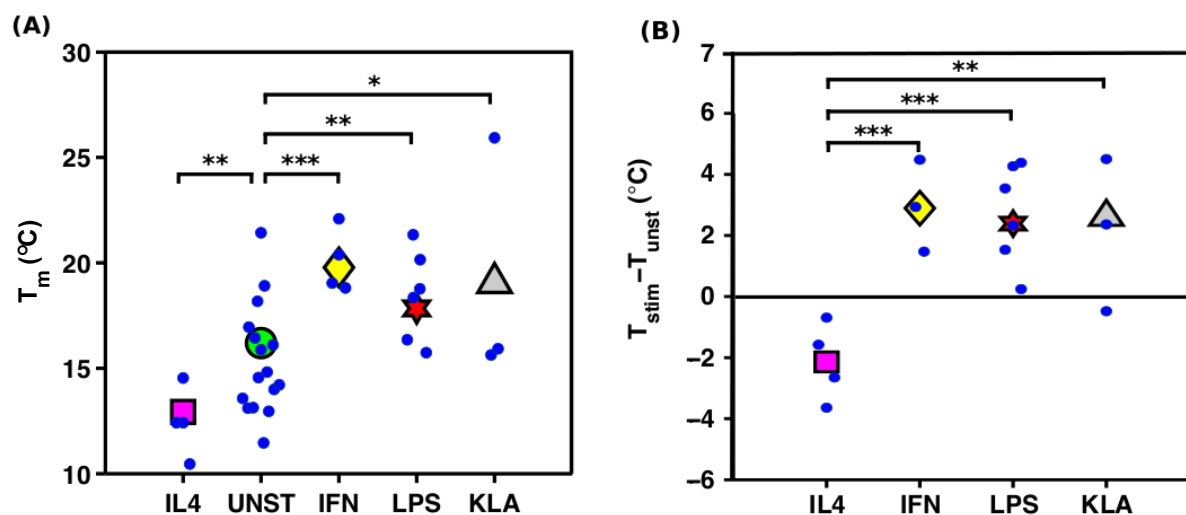


**Figure 3. Pro- and anti-inflammatory treatments affect the transition temperature systematically.** The scatter in the absolute transition temperature (particularly notable in the unstimulated UNST cells) is reduced significantly comparing with same-day unstimulated controls. (A): Fitted transition temperatures of vesicles produced by macrophage cells treated with IL4, IFN- $\gamma$ , LPS or Kdo-LipidA for 12 hours. Each small data marker comes from an experiment with between 300 and 600 vesicles. The large markers indicate the average in each distribution, weighted with the errors on  $T_m$ . (B): Temperature difference of each stimulation experiment with its control condition. From one-way analysis of variance (ANOVA) we obtained the distributions differences to be statistically significant with \*  $p < 0.1$ , \*\*  $p < 0.05$ , \*\*\*  $p < 0.005$ .

### 136 Isolation of Lipids, and Gel-assisted vesicles formation

137 For the lipids isolation procedure we followed the Bligh and Dyer method *Bligh and Dyer (1959)*: 1 ml  
 138 of GPMVs sample is collected and moved to a vial. Then are added 3.75 ml of 1:2 chloroform and  
 139 methanol mixture, 1.25 ml of chloroform and 1.25 ml of distilled water. After each step the solution  
 140 is vortexed for 1 minute. At this stage the GPMVs burst and the components dissolve in the solution.  
 141 The mixture is then centrifuged at 1000 RPM for 5 minutes. This makes the chloroform/methanol  
 142 fraction deposit at the bottom of the tube, together with the lipids, while the aqueous and water  
 143 soluble component is isolated at the top. Proteins are preferentially located at the interface between  
 144 the two phases. The bottom phase is then collected and left under vacuum to let the solvents  
 145 evaporate. Finally lipids are redissolved in 100  $\mu$ l of chloroform.

146 The vesicles are produced through the gel-assisted method as described in *Weinberger et al.*  
 147 (2013): 200  $\mu$ l of 5% (weight/weight) PVA solution is spread on a microscope coverslip with the help  
 148 of a spincoater and then left to dry in an oven at 50°C for 30 minutes. Lipids dissolved in 100  $\mu$ l  
 149 of chloroform are then spread on PVA gel. A chamber is formed with the help of a spacer and a  
 150 second coverslip and filled with a solution of sucrose. After 30 minutes the vesicles are collected  
 151 and diluted in glucose solution to allow vesicle sedimentation.

### 152 Imaging

153 The samples are imaged on a Nikon Eclipse Ti-E inverted epifluorescence microscope using a Nikon  
 154 PLAN APO 40 $\times$  0.95 N.A. dry objective and a IIDC Point Grey Research Grasshopper-3 camera.  
 155 The perfect focus system (Nikon) maintains the sample in focus even during thermal shifts. The  
 156 temperature of the sample is controlled with a home-made computer-controlled Peltier device. A  
 157 thermocouple is placed in direct contact with the sample chamber. In each position a z-stack of  
 158 8 images is acquired, spanning across a range similar to the bleb size. The temperature is decreased  
 159 across the whole sample with a ramp from 37 to 3°C in steps of 2°C; at each step the temperature is  
 160 let to equilibrate for 15 seconds. The abundance of GPMVs produced can vary from cells prepared  
 161 in different days, but usually from a dish of 5.5 cm diameter with confluent cells it is possible to  
 162 produce blebs for at least 2 experiments. With the quantities described above, we are able to image  
 163 up to 100-200 blebs in each field of view.

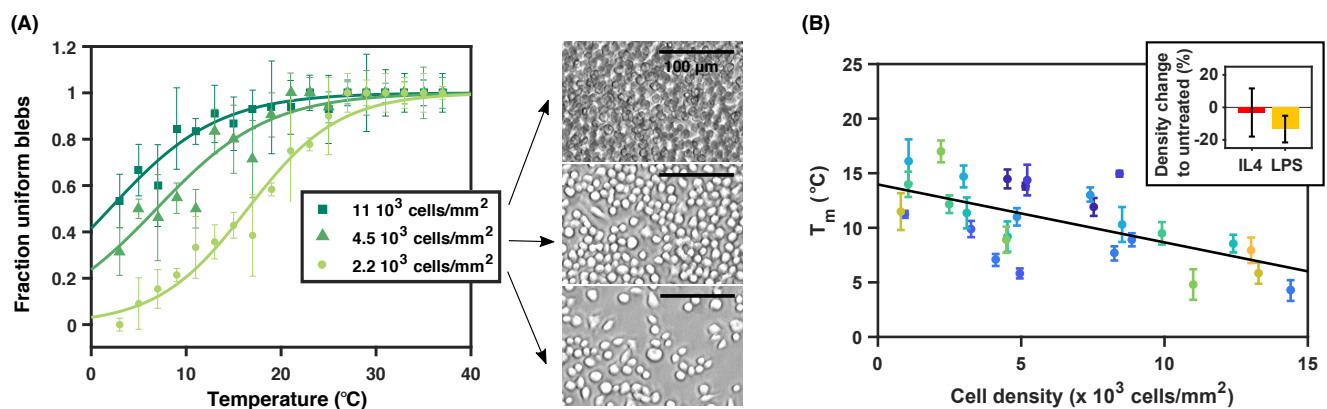


**Figure 4. Cell crowding affects the phase transition of GPMVs.** (A) There is a consistent shift in the data for the fraction of uniform GPMVs, from cell cultures at different densities.  $T_{11} = (4.8 \pm 1.4)^{\circ}\text{C}$ ,  $T_{4.5} = (8.9 \pm 1.2)^{\circ}\text{C}$ ,  $T_{2.2} = (17.0 \pm 1.0)^{\circ}\text{C}$ . (B) The miscibility temperatures obtained from the sigmoidal curve fitting, as a function of the cell crowding, showing that the denser samples have lower transition temperature. Same colors indicate repetition of the experiment on same day. The linear fit  $y = a + cx$  gives  $c = (-0.53 \pm 0.26)^{\circ}\text{C mm}^2/\text{cells}$  and  $a = (14.0 \pm 1.9)^{\circ}\text{C}$ . In the sub-panel is represented the density change as effect of 12 hours of stimulation compared to an untreated sample at our typical experiment densities ( $7 \cdot 10^3$  cells/ $\text{mm}^2$ ). Numerical values obtained over 4 repetitions are:  $(-3 \pm 15)\%$  for IL4 treated, and  $(-13 \pm 8)\%$  for LPS treated.

**Figure 4–Figure supplement 1.** Miscibility temperature of three repetitions of the same experiment in which macrophage cells at the same density are cultured in three separate flasks as replicates for two days. The data points have a wide temperature range both within the replicates and comparing the three experiments. Data points are also interpreted as representative of a whole distribution with the same average and standard deviation. In spite of the large variation, the sum of the distributions shows a main peak around  $13^{\circ}\text{C}$ . Continuous distributions are obtained simulating gaussian distributed numbers with mean and standard deviation equal to the value of the data and their error.

**Figure 4–Figure supplement 2.** Control experiment to test the effect of intracellular communication through secretion of cytokines on the melting temperature of GPMVs. The two samples were plated at the same density, and blebbing was induced after 12 hours during which the medium of the "washed" sample was changed every two hours. The control sample shows a lower  $T_m$  compared to the "washed", see Figure 4-supplement 2. This is compatible with a scenario in which the control condition is affected by an accumulation of M2-inducing cytokines like IL4.  $T_{control} = 5.8 \pm 1.0$ ,  $T_{washed} = 7.9 \pm 1.2$

## 164 Software processing

165 A custom Matlab software pipeline has been developed to automatically detect the position and  
 166 radius of the GPMVs in the images. It uses the Hough transform to detect circular features. Then  
 167 with the help of a graphical user interface the blebs are shown to the user one at the time, the  
 168 user can interactively scroll the z-stack and decide if the bleb shows (a) a single phase, (b) phase  
 169 coexistence or (c) unclear phenotype. The software randomly picks the vesicle to show, from the  
 170 database of all the temperatures, i.e. in this stage the information about the temperature is kept  
 171 hidden to the user, so that the decision process (assigning the type a/b/c) is unbiased.

## 172 Results

173 Following established protocols, GPMVs are produced from macrophage cells using PFA and DTT.  
 174 The sample is observed under an optical microscope and it is in contact with a temperature control  
 175 system. The temperature is lowered from 37 to  $3^{\circ}\text{C}$  in steps of  $2^{\circ}\text{C}$ . At high temperatures all the  
 176 vesicles show a uniform phase. Around  $12\text{--}22^{\circ}\text{C}$  phase separation domains start to appear in some  
 177 GPMVs, and at low temperatures most of the GPMVs are phase separated (see Figure 1 A). For  
 178 each temperature we calculate the fraction  $f(T)$  of GPMVs which show uniform phase or phase  
 179 separation. Before producing GPMVs, macrophages are stimulated with one of IFN, LPS or KLA for  
 180 12 hours to induce pro-inflammatory response. In each data set (Figure 1 B-E) we compare the  
 181 stimulated condition with its unstimulated control data set, since we noticed (as has been already  
 182 reported in different cell types *Gray et al. (2013, 2015)*) a significant variability in the transition  
 183 temperature of independent repeats; in contrast, the transition temperatures of GPMVs from the  
 184 same cultures, even split into separate dishes, are tightly distributed.

185 The transition temperature  $T_m$  is obtained by fitting the  $f(T)$  data with an empirical sigmoidal  
186 curve:

$$f(T) = A \left[ \tanh \left( \frac{T - T_m}{\sigma} \right) + 1 \right] + C, \quad (1)$$

187 where  $T_m$  and  $\sigma$  are the most interesting parameters to describe the mean and the cell-to-cell  
188 variability (GPMVs originate from individual cells) in the transition temperature of the population.  
189 Error bars are associated with data points by randomly separating the measurements for a given  
190 temperature into three groups, and treating these as independent data sets.

191 Figure 1 B shows the effect of the cell stimulation with KLA for 12 hours. The comparison  
192 with the control condition shows a shift of 4.5°C in the GPMVs transition temperature to higher  
193 temperatures. As expected, LPS and KLA stimulations produce similar effects (see Figure 1 B-C).  
194 Indeed Kdo-LipidA is the active sub-unit of the LPS molecule which is recognized by the TLR4  
195 trans-membrane receptor *Park et al. (2009)*. Notice that the comparison between LPS and KLA has  
196 to remain qualitative since there isn't a first-principles way to correlate the doses, except for the  
197 effects on activating cells. Both doses employed here are known to be able to saturate the cell  
198 response, for example in terms of TNF $\alpha$  production *Andreyev et al. (2010)*; *Vasan et al. (2007)*. As a  
199 control, repeating the same experiment of KLA stimulation, this time on TLR4<sup>-/-</sup> macrophage cells,  
200 we obtained compatible transition trends (Figure 1 D) between the stimulated and unstimulated  
201 condition. This confirms that the observed temperature shift is originated from the metabolic  
202 change as a downstream effect of triggering NF- $\kappa$ B signalling, more than any other spurious effect.  
203 We then stimulated cells with IFN- $\gamma$ , known, like LPS, to have pro-inflammatory effects *Martinez*  
204 *and Gordon (2014)*, and obtained the same qualitative effect on the plasma membrane transition  
205 temperature (Figure 1 E).

206 Since all the experiments with the "classically activated" conditions were showing a consistent  
207 shift in the same direction, we decided to stimulate the cells with interleukin-4 (IL4) which is known  
208 to induce a different type of differentiation *Mosser and Edwards (2008)*. Macrophages treated with  
209 IL4 have different phenotypes and markers compared to the M1, and a different role in the immune  
210 response: they don't produce pro-inflammatory cytokines, but suppress destructive immunity, and  
211 are involved for example in wound healing response *Mosser and Edwards (2008)*. The curves in  
212 Figure 2 correspond to the control condition and to 24 hours of IL-4 stimulation. Also in this case  
213 the stimulation produces a temperature shift, but in contrast to the "classically activated" cells, in  
214 this case the  $T_m$  shifts towards lower temperatures.

215 Collecting together all the  $T_m$  values from different stimulation experiments (see Figure 3 A) we  
216 can see how the IL4 data and the IFN- $\gamma$ /LPS/KLA data are in two separate temperature ranges, with  
217 no data overlapping, while the values from the unstimulated experiments have a much wider range.  
218 Statistical analysis confirms the distributions to be significantly different ( $p < 0.05$ ) for almost all of  
219 the conditions. Calculating the temperature differences  $T_{stim} - T_{unstim}$  for all the 12 hours stimulation  
220 experiments (i.e. comparing with same day controls), the temperature shifts tighten (Figure 3 B)  
221 and show very consistent behaviors: the IL4 data points are all negative, whereas the others are all  
222 positive.

223 We then investigated cell density as one of the possible causes for the large variability of  $T_m$  in  
224 the control condition. For the experiments described above, we used a cellular concentration from  
225 about 6 to 7·10<sup>3</sup> cells/mm<sup>2</sup>. The effectiveness of intracellular communication indeed depends on  
226 the cell density, and can be conveyed through both mechanical or chemical interaction *Stow et al.*  
227 *(2009)*; *Fortes et al. (2004)*; *Lim et al. (2011)*. In Figure 4 we report the results of experiments done  
228 growing cells in a common flask, and then plated at different densities. The transition temperature  
229 correlates with the cell density, so that the curve that corresponds to the most crowded sample is  
230 on the right of the less dense samples (see Figure 4 A). Summarizing all the density measurements,  
231 we obtain a linear trend of the miscibility temperature as a function of the cell density (Figure 4 B). A  
232 similar trend has been obtained recently in similar experimental conditions for other cell types *Gray*  
233 *et al. (2015)*, and possible causes are presented in the discussion.

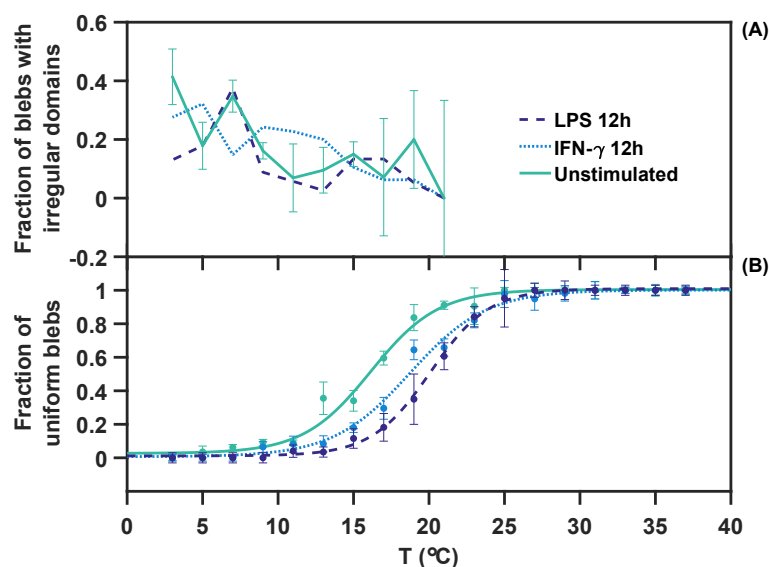


**Figure 5. At very low temperatures, irregular shaped domains are observed and attributed to a gel phase.** (A) The fraction of GPMVs with irregular domains (over the total of phase separated GPMVs) increases at low temperatures. This fraction grows below  $T_m$ , as can be seen comparing in (B) the 'conventional' data on liquid-liquid phase separation for the three conditions indicated in the legend.

**Figure 5-Figure supplement 1.** Example GPMVs showing round domains (A) and an irregular domain (B). These different shapes likely correspond respectively to liquid-liquid and liquid-gel phase coexistence.

234 We had at this point to check the possibility that the temperature shift observed as a function  
235 of the pro/anti-activation treatment might be an indirect effect, due to a differential stimulus-  
236 dependent growth. To check for this, we measured cell growth through the difference in cell density  
237 after IL4 and LPS stimulation. Reproducing our typical experimental conditions ( $7 \cdot 10^3$  cells/mm<sup>2</sup>, and  
238 12 h stimulation), we obtained a non-significant change in the density of IL4 treated cells compared  
239 to the unstimulated condition, while the LPS showed a decrease of 13%. Putting together the  
240 growth rate reduction with LPS with the calibrated cell-concentration results, for the LPS condition  
241 we obtain (as an indirect effect of the stimulant on the cell culture growth rate) an expected change  
242 of the melting temperature of about  $-0.5^\circ\text{C}$  compared to the untreated condition. Therefore this  
243 important control shows that the  $\sim 2$  degrees difference in  $T_m$  seen between untreated and LPS  
244 stimulated is due only in small part to cell density, so most of the effect has to be accounted for by  
245 processes independent of density, downstream of the LPS signalling pathway.

246 The high quality imaging allowed us to investigate also the shape of the phase separation  
247 domains appearing in blebs at low temperatures. Some of the domains indeed appear to have  
248 an irregular rigid shape similar to a gel phase domain, while others look more rounded like in the  
249 situation of liquid-liquid coexistence. With the help of a graphical user interface that shows a 3-4  
250 frames time sequence of the vesicle, GPMVs with irregular domains were identified as the one  
251 presenting rigid and not rounded dark regions (see Figure 5-supplement 1). The appearance of gel  
252 looking domains on GPMVs has already been reported *Gray et al. (2015)*, but this is the first attempt  
253 for a quantification of the phenomenon. Three sets of data in different conditions are shown in  
254 Figure 5. In all the cases, in spite of the noise, the fraction of irregular domains over the total of  
255 phase separated GPMVs has a clear growth at low temperatures, reaching about 0.4 at  $3^\circ\text{C}$ . On the  
256 other hand we don't see any significant difference in these trends comparing different stimulation  
257 conditions. In the event that these irregular domains could be confirmed as gel domains, this kind  
258 of analysis would provide an additional piece of information on the phase diagram of the biological  
259 membrane lipid mixture (on which we don't have almost any knowledge) and might be particularly



260 important in cell biology regulation involving cholesterol *Ayuyan and Cohen (2018)*.

261 The experiments described so far provide evidence that the composition of the plasma mem-  
262 brane is regulated according to the external milieu, but we still don't know if this change involves  
263 just the lipids and/or also the membrane protein composition or abundance. To address this, we  
264 performed an important and seldom considered control: comparing the melting temperature of  
265 GPMVs with the same sample after a lipid purification process. The GPMVs sample was divided  
266 in two aliquots, and one of them was dissolved, purified and the vesicles re-formed through the  
267 gel-assisted formation technique, as described in the methods section. The two samples are found  
268 to have compatible values for their miscibility temperature (see Figure 6 and Figure 6-supplement 1),  
269 meaning that the phase separation phenomenon on GPMVs is lipid driven and that the miscibility  
270 temperature is mostly unperturbed by membrane proteins. It is also worth remarking that these  
271 reconstituted vesicles have lost any possible bilayer asymmetry maintained in the GPMVs.

## 272 Discussion

273 It is well known that the plasma membrane is not just a passive support for activity by membrane  
274 proteins, and here we have developed the theme that the property of lipids to phase segregate  
275 relates to protein interactions *Veatch and Cicuta (2018)*; *Kimchi et al. (2018)*. GPMVs are an ex-  
276 tremely useful system to understand this aspect of plasma membranes because they maintain  
277 the composition of the original membrane, but they can be studied as an isolated structure and  
278 subjected to stringent controls. Our results add to the body of evidence that proximity to the critical  
279 point for phase separation can be a global regulator favoring activity, and for the specific case of  
280 macrophage cell activation our results are consistent with previous findings that the early stages of  
281 TLR4 activation take place in raft domains *Triantafilou et al. (2002)*.

## 282 Effect of stimulation on plasma membrane transition temperature

283 We have seen how treatment of macrophages with different stimulating agents affects the melting  
284 temperature of GPMVs. All the stimulants used (IFN- $\gamma$ , LPS, KLA, and IL4) induced a shift of few  
285 degrees compared to the control condition, meaning that in all the cases the membrane composition  
286 has changed as a consequence of the activation of specific signaling pathways. Moreover, IFN- $\gamma$ , LPS  
287 and KLA increased the transition temperature ( $T_m$ ), whereas IL4 had the opposite effect decreasing  
288  $T_m$ . Given that the first three stimulants can be connected to the activation into the M1 state  
289 in macrophages, whereas IL4 is responsible for the differentiation into the M2 state, this result  
290 sheds new light on the importance of plasma membrane composition in the immune response,  
291 and suggests new ways in which lipidomics may be involved in the regulation of the host defense  
292 strategy.

293 From the point of view of the membrane composition, if the melting temperature increases  
294 (coming closer to physiological temperature) it means that spontaneous lipid domains are longer  
295 lived and larger, so that membrane components can partition more strongly; also, the energy cost to  
296 recruit a particular lipid micro-environment around a protein is reduced *Kimchi et al. (2018)*. It has  
297 been calculated that due to this universal phenomenon, the proximity to critical point, spontaneous  
298 lipid domains exist at sizes of around 22 nm for GPMVs from RBL cells *Veatch et al. (2008)*. This  
299 argument considers the dimension of the correlation length  $\xi$  at a physiological temperature ( $T =$   
300  $37^\circ\text{C}$ ), and experiments that measured  $T_m$ , then using the expression  $\xi = \xi_o T_m / (T - T_m)$  *Honerkamp-*  
301 *Smith et al. (2008)*. This same argument can now be extended, in light of the results presented  
302 here: keeping the same value of  $\xi_o$  from *Veatch et al. (2008)* (because this is a quantity linked to the  
303 size of the lipid) we can estimate the effect of an increase in  $T_m$  from  $T_{m\ M1} = 13$  to  $T_{m\ M2} = 20^\circ\text{C}$   
304 (as from figure 3). This results in an increase of the correlation length of the order of 40% (from  
305  $\xi_{M1} = 12$  to  $\xi_{M2} = 17$  nm). We expect this to have effect on confinement of proteins and their local  
306 concentration, and thus to affect for in the particular system here the balance of dimerisation in  
307 TLR4 receptors, and hence regulate the initiation of signaling pathways.

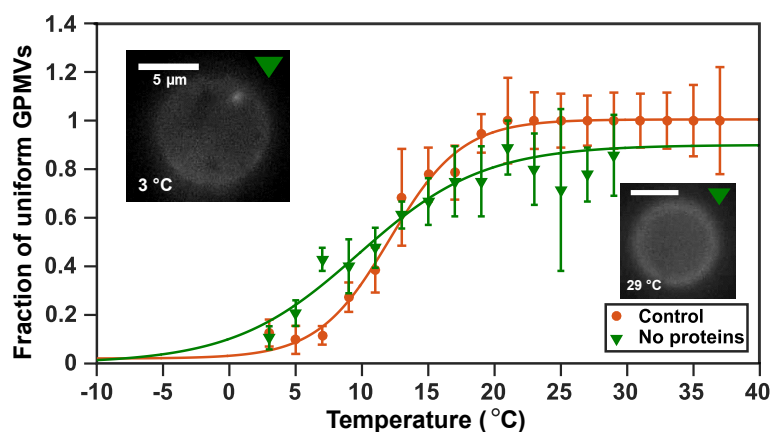


**Figure 6. A key control with purified lipids excludes the role of proteins in the phenomena reported above.** Comparison between the distribution of uniform GPMVs against analysis of vesicles re-formed from the just the lipidic component purified from the same sample. The melting temperature is compatible, within the error, meaning that the lipids are unperturbed in the determination of the melting temperature.  $T_{no\ proteins} = (11.1 \pm 1.4)^{\circ}C$ ,  $T_{control} = (12.2 \pm 0.5)^{\circ}C$ .

**Figure 6-Figure supplement 1.** In the same way as the ‘parent’ GPMV, it has been checked that vesicles reformed from just the lipid fraction purified from GPMVs undergo phase separation. The images show phase separation (dark domains) appearing at 18 and 12°C.

### 308 Speculative correlation between membrane composition and receptor activity

309 We suggest here a possible correlation between the role of the cell in the immune defense and  
 310 the changes in its membrane composition. One can imagine that these cells, depending on their  
 311 activation state, regulate their lipid composition in such a way to tune the proximity to the critical  
 312 point, and hence in turn the typical dimension and lifetime of spontaneous lipid domains, in  
 313 order to be more or less reactive towards external stimuli. An M1 cell would have bigger and  
 314 more long-lasting lipid domains, leading to increased activity of TLR4 receptors, which have raft  
 315 affinity *Plóciennikowska et al. (2014)*; *Triantafilou et al. (2002)*; *Pfeiffer et al. (2001)*; *Triantafilou*  
 316 *et al. (2004)* (e.g. by increased recruitment to the membrane, and increased dimerization), to  
 317 induce a faster and stronger inflammatory response with consequent production of inflammatory  
 318 cytokines. In contrast, in M2 cells the activation of the TLR4 to NF- $\kappa$ B pathway would be down-  
 319 regulated through the lipid composition effect. An important element in support of this hypothesis  
 320 is the reported increased sensitivity to LPS after IFN- $\gamma$  treatment, both in mice *Matsumura and*  
 321 *Nakano (1988)* and in macrophages in vitro *Darmani et al. (1994)*, where a 66% increase of the LPS  
 322 binding efficiency has been measured.

### 323 Effect of cell density on $T_m$

324 We see a shift of  $T_m$  with cell density. One could relate this result with the shift given by the  
 325 different kind of stimulations, venturing a picture in which the overcrowded populations have  
 326 some common behavior with M2 cells. In this picture, the crowded populations, with no need to  
 327 further recruit cells and promote additional inflammation against possible infections, diminish their  
 328 cytokine production, thus acting more like M2 cells. This hypothesis is supported by the observation  
 329 that BMDMs from high density cultures secrete less pro-inflammatory cytokines and have lower  
 330 phagocytic ability *Lee and Hu (2013)*. Moreover the number of cells showing typical M2 membrane  
 331 markers like CD11c and Ly-6CLy-6G increases in dense cultures *Lee and Hu (2013)*.

332 A second mechanism could be identified in the asymmetry in the exposed membrane at different  
 333 densities. Indeed at high densities the only region of the cell exposed is the top surface while the  
 334 neighbor cell hide the lateral sides. The vesicles forming from the free surface could therefore be  
 335 affected by the differences in the membrane composition due to the basal/apical polarization. To  
 336 test the hypothesis of the interaction through cytokines, we performed an experiment where the

337 medium was periodically changed every 2 hours. This treatment did not produce a significant  
338 change in  $T_m$  (see Figure in Supplementary Materials), meaning that the density effect is mainly due  
339 to interaction through mechanical contact.

340 Even though the density has been proven to be an important factor in the day-to-day variability  
341 in the  $T_m$  of unstimulated macrophages, this is not enough to explain the variability between  
342 independent repeats, indeed just keeping the cells in separate cultures is enough to produce some  
343 variability (Figure 4-supplement 1). To investigate the cause of the  $T_m$  day-to-day variation, the  
344 effect of cell density was tested, and the results showed that denser populations gave a lower  $T_m$  in  
345 GPMVs. The same experiment has been very recently performed on rat basophilic leukemia cells  
346 (RBL) *Gray et al. (2015)* with the same outcome, the authors suggesting that dense populations  
347 could have different physical membrane properties to be able to sense and communicate with  
348 touching cells *Frechin et al. (2015)*. Our hypothesis is that cell density indirectly induces a decrease  
349 in  $T_m$ , perhaps by triggering the production of cytokines with the same effect of IL4. This picture is  
350 supported by a study in which M1/M2-like differentiation was induced by the population density *Lee*  
351 *and Hu (2013)*. Indeed, among other things, denser cell cultures were found less efficient in the  
352 production of cytokines than sparser ones after LPS stimulation *Lee and Hu (2013)*. We tested this  
353 hypothesis comparing the  $T_m$  of two samples plated at the same density. GPMVs were produced  
354 after 12 hours, but during this time in one of the samples we changed the medium every 2 hours.  
355 This "washed" sample shows a higher  $T_m$  compared to the control, where cytokines would be  
356 accumulating in the medium, see Figure 4-supplement 2. This is compatible with a scenario in  
357 which the control condition is affected by an accumulation of M2-inducing cytokines such as IL4.

## 358 Conclusions

359 For the first time, vesicles from purely the lipid fraction of GPMV from plasma membrane of  
360 macrophages have been observed, and their phase behaviour compared to the GPMV. This showed  
361 that both form phase separated domains on cooling, that the composition is close to a critical point,  
362 and that the melting temperature is unaffected by the presence of proteins. Also for the first time,  
363 we quantified the fraction of irregular domains on GPMVs, observing an increase of these at low  
364 temperatures. These are likely to be general results common to plasma membrane compositions in  
365 many cell types. The main biological question addressed here concerns macrophage cells, which  
366 we conditioned via pro- and anti-inflammatory stimuli, before extracting GPMV and measuring the  
367 phase transition temperatures. Considering all the transition temperatures together we get a very  
368 consistent picture: transition temperatures following IL4, as opposed to IFN- $\gamma$ /LPS/KLA treatment,  
369 form two non-overlapping intervals (respectively at 10-15°C and 15-25°C). The absolute temperature  
370 changes induced by stimulation are always around 2°C compared to control. We have described  
371 a physical mechanism that can underpin this correlation between the immune response role of  
372 macrophage cells and the lipid composition of their plasma membranes, where signaling activation  
373 initiates. Much remains to be discovered within the 'critical lipidomics' paradigm, specifically direct  
374 experiments are becoming possible thanks to superresolution approaches *Stone et al. (2017)*;  
375 *Veatch and Cicuta (2018)*; *Brandtsma et al. (2018)*, probing membrane protein copy numbers and  
376 states of aggregation and how these are affected by the proximity to lipid mixture critical points.

## 377 Acknowledgments

378 Research was funded by EU Marie Curie action ITN TransPol (EC), NIH-R01GM110052 and NSF-  
379 MCB1552439 (SLV), Cambridge University Commonwealth, European and International Trust (JS)  
380 and ITN BioPol (PC), Wellcome Trust Investigator grant 08045/Z/15/Z (CEB).

## 381 References

382 *Akira S, Takeda K. Toll-like receptor signalling. Nat Rev Immunol. 2004; 4:499-511.*

- 383 **Andreyev AY**, Fahy E, Guan Z, Kelly S, Li X, McDonald JG, Milne S, Myers D, Park H, Ryan A, Thompson BM, Wang  
384 E, Zhao Y, Brown HA, Merrill AH, Raetz CRH, Russell DW, Subramaniam S, Dennis EA. Subcellular organelle  
385 lipidomics in TLR-4-activated macrophages. *J Lipid Res.* 2010; 51:2785–2797.
- 386 **Ayuyan AG**, Cohen FS. The Chemical Potential of Plasma Membrane Cholesterol: Implications for Cell Biology.  
387 *Biophys J.* 2018; 114:904–918.
- 388 **Bach EA**, Aguet M, Schreiber RD. The IFN  $\gamma$  Receptor: A Paradigm for Cytokine Receptor Signaling. *Ann Rev*  
389 *Immunol.* 1997; 15:563–591.
- 390 **Baumgart T**, Hammond AT, Sengupta P, Hess ST, Holowka DA, Baird BA, Webb WW. Large-scale fluid/fluid  
391 phase separation of proteins and lipids in giant plasma membrane vesicles. *Proc Natl Acad Sci.* 2007;  
392 104(9):3165–3170.
- 393 **Blakney AK**, Swartzlander MD, Bryant SJ. The effects of substrate stiffness on the in vitro activation of  
394 macrophages and in vivo host response to poly(ethylene glycol)-based hydrogels. *J Biomed Mater Res*  
395 *A.* 2012; 100:1375–1386.
- 396 **Bligh EG**, Dyer WJ. A Rapid Method of Total Lipid Extraction and Purification. *Canadian J Biochem Physiol.* 1959;  
397 37:911–917.
- 398 **Brandsma AM**, Schwartz SL, Wester MJ, Valley CC, Blezer GLA, Vidarsson G, Lidke KA, Ten Broeke T, Lidke DS,  
399 Leusen JHW. Mechanisms of inside-out signaling of the high-affinity IgG receptor Fc $\gamma$ RI. *Sci Signal.* 2018;  
400 11:eaq0891.
- 401 **Bryant CE**, Spring DR, Gangloff M, Gay NJ. The molecular basis of the host response to lipopolysaccharide. *Nat*  
402 *Rev Micro.* 2010 Jan; 8:8–14.
- 403 **Burns M**, Wissner K, Wu J, Levental I, Veatch SL. Miscibility Transition Temperature Scales with Growth Temperature  
404 in a Zebrafish Cell Line. *Biophys J.* 2017; 113:1212–1222.
- 405 **Darmani H**, Parton J, Harwood JL, Jackson SK. Interferon-gamma and polyunsaturated fatty acids increase the  
406 binding of lipopolysaccharide to macrophages. *Int J Exp Pathol.* 1994; 75:363–368.
- 407 **Dennis EA**, Deems RA, Harkewicz R, Quehenberger O, Brown HA, Milne SB, Myers DS, Glass CK, Hardiman G,  
408 Reichart D, Merrill AH, Sullards MC, Wang E, Murphy RC, Raetz CRH, Garrett TA, Guan Z, Ryan AC, Russell DW,  
409 McDonald JG, et al. A Mouse Macrophage Lipidome. *J Biol Chem.* 2010; 285:39976–39985.
- 410 **Fortes FSA**, Pecora IL, Persechini PM, Hurtado S, Costa V, Coutinho-Silva R, Braga MBM, Silva-Filho FC, Bisaggio  
411 RC, Farias FPd, Scemes E, Carvalho ACCd, Goldenberg RCS. Modulation of intercellular communication in  
412 macrophages: possible interactions between GAP junctions and P2 receptors. *J Cell Sci.* 2004; 117:4717–4726.
- 413 **Frechin M**, Stoeger T, Daetwyler S, Gehin C, Battich N, Damm EM, Stergiou L, Riezman H, Pelkmans L. Cell-  
414 intrinsic adaptation of lipid composition to local crowding drives social behaviour. *Nature.* 2015; 523:88–91.
- 415 **Fridriksson EK**, Shipkova PA, Sheets ED, Holowka D, Baird B, McLafferty FW. Quantitative Analysis of Phospho-  
416 lipids in Functionally Important Membrane Domains from RBL-2H3 Mast Cells Using Tandem High-Resolution  
417 Mass Spectrometry. *Biochem.* 1999; 38:8056–8063.
- 418 **Goral J**, Kovacs EJ. In Vivo Ethanol Exposure Down-Regulates TLR2-, TLR4-, and TLR9-Mediated Macrophage  
419 Inflammatory Response by Limiting p38 and ERK1/2 Activation. *J Immunol.* 2005; 174:456–463.
- 420 **Gray E**, Karlake J, Machta BB, Veatch SL. Liquid General Anesthetics Lower Critical Temperatures in Plasma  
421 Membrane Vesicles. *Biophys J.* 2013; 105:2751–2759.
- 422 **Gray EM**, Díaz-Vázquez G, Veatch SL. Growth Conditions and Cell Cycle Phase Modulate Phase Transition  
423 Temperatures in RBL-2H3 Derived Plasma Membrane Vesicles. *PLoS ONE.* 2015; 10:e0137741.
- 424 **Honerkamp-Smith A**, Cicuta P, Collins MD, Veatch SL, den Nijs M, Schick M, Keller SL. Line tensions, correlation  
425 lengths, and critical exponents in lipid membranes near critical points. *Biophys J.* 2008; 95:236–246.
- 426 **Honigsmann A**, Sadeghi S, Keller J, Hell SW, Eggeling C, Vink R. A lipid bound actin meshwork organizes liquid  
427 phase separation in model membranes. *eLife Sciences.* 2014 Mar; 3:e01671.
- 428 **Hoshino K**, Takeuchi O, Kawai T, Sanjo H, Ogawa T, Takeda Y, Takeda K, Akira S. Cutting Edge: Toll-Like Receptor 4  
429 (TLR4)-Deficient Mice Are Hyporesponsive to Lipopolysaccharide: Evidence for TLR4 as the Lps Gene Product.  
430 *J Immunol.* 1999; 162:3749–3752.

- 431 **Kaiser HJ**, Lingwood D, Levental I, Sampaio JL, Kalvodova L, Rajendran L, Simons K. Order of lipid phases in  
432 model and plasma membranes. *Proc Natl Acad Sci USA*. 2009 Sep; 106:16645–16650.
- 433 **Kawai T**, Akira S. The role of pattern-recognition receptors in innate immunity: update on Toll-like receptors.  
434 *Nat Immunol*. 2010; 11:373–384.
- 435 **Kigerl KA**, Gensel JC, Ankeny DP, Alexander JK, Donnelly DJ, Popovich PG. Identification of Two Distinct  
436 Macrophage Subsets with Divergent Effects Causing either Neurotoxicity or Regeneration in the Injured  
437 Mouse Spinal Cord. *J Neurosci*. 2009; 29:13435–13444.
- 438 **Kimchi O**, Veatch SL, Machta BB. Ion channels can be allosterically regulated by membrane domains near a  
439 de-mixing critical point. *J Gen Physiol*. 2018; 150:1769–1777.
- 440 **Lawrence T**, Natoli G. Transcriptional regulation of macrophage polarization: enabling diversity with identity.  
441 *Nat Rev Immunol*. 2011 Nov; 11:750–761.
- 442 **Lee CM**, Hu J. Cell density during differentiation can alter the phenotype of bone marrow-derived macrophages.  
443 *Cell & Bioscience*. 2013; 3:30.
- 444 **Lim TS**, Mortellaro A, Lim CT, Hämmerling GJ, Ricciardi-Castagnoli P. Mechanical Interactions between Dendritic  
445 Cells and T Cells Correlate with T Cell Responsiveness. *J Immunol*. 2011 Jul; 187:258–265.
- 446 **Martinez FO**, Gordon S. The M1 and M2 paradigm of macrophage activation: time for reassessment.  
447 *F1000Prime Rep*. 2014 Mar; 6.
- 448 **Matsumura H**, Nakano M. Endotoxin-induced interferon-gamma production in culture cells derived from  
449 BCG-infected C3H/HeJ mice. *J Immunol*. 1988 Jan; 140:494–500.
- 450 **Mosser DM**, Edwards JP. Exploring the full spectrum of macrophage activation. *Nat Rev Immunol*. 2008;  
451 8:958–969.
- 452 **Nakahira K**, Kim HP, Geng XH, Nakao A, Wang X, Murase N, Drain PF, Wang X, Sasidhar M, Nabel EG, Takahashi  
453 T, Lukacs NW, Ryter SW, Morita K, Choi AMK. Carbon monoxide differentially inhibits TLR signaling pathways  
454 by regulating ROS-induced trafficking of TLRs to lipid rafts. *J Exp Med*. 2006; 203:2377–2389.
- 455 **Park BS**, Song DH, Kim HM, Choi BS, Lee H, Lee JO. The structural basis of lipopolysaccharide recognition by the  
456 TLR4-MD-2 complex. *Nature*. 2009; 458:1191–1195.
- 457 **Pfeiffer A**, Böttcher A, Orsó E, Kapinsky M, Nagy P, Bodnár A, Spreitzer I, Liebisch G, Drobnik W, Gempel K,  
458 Horn M, Holmer S, Hartung T, Multhoff G, Schütz G, Schindler H, Ulmer AJ, Heine H, Stelter F, Schütt C, et al.  
459 Lipopolysaccharide and ceramide docking to CD14 provokes ligand-specific receptor clustering in rafts. *Eur J*  
460 *Immunol*. 2001; 31:3153–3164.
- 461 **Plóciennikowska A**, Hromada-Judycka A, Borzęcka K, Kwiatkowska K. Co-operation of TLR4 and raft proteins in  
462 LPS-induced pro-inflammatory signaling. *Cell Mol Life Sci*. 2014 Oct; 72:557–581.
- 463 **Pralle A**, Keller P, Florin EL, Simons K, Hörber JKH. Sphingolipid-Cholesterol Rafts Diffuse as Small Entities in the  
464 Plasma Membrane of Mammalian Cells. *J Cell Biol*. 2000; 148:997–1008.
- 465 **Pruett SB**, Zheng Q, Fan R, Matthews K, Schwab C. Acute exposure to ethanol affects Toll-like receptor signaling  
466 and subsequent responses: an overview of recent studies. *Alcohol*. 2004; 33:235–239.
- 467 **Pruett SB**, Zheng Q, Fan R, Matthews K, Schwab C. Ethanol suppresses cytokine responses induced through  
468 Toll-like receptors as well as innate resistance to *Escherichia coli* in a mouse model for binge drinking. *Alcohol*.  
469 2004 Jun; 33:147–155.
- 470 **Scott RE**. Plasma membrane vesiculation: a new technique for isolation of plasma membranes. *Science*. 1976  
471 Nov; 194:743–745.
- 472 **Scott RE**, Maercklein PB. Plasma membrane vesiculation in 3T3 and SV3T3 cells. II. Factors affecting the process  
473 of vesiculation. *J Cell Sci*. 1979; 35:245–252.
- 474 Sens P, Bassereau P, editors. *Physics of Biological Membranes*. Springer; 2018.
- 475 **Sezgin E**, Kaiser HJ, Baumgart T, Schwille P, Simons K, Levental I. Elucidating membrane structure and protein  
476 behavior using giant plasma membrane vesicles. *Nat Protocols*. 2012; 7:1042–1051.
- 477 **Simons K**, Sampaio JL. Membrane Organization and Lipid Rafts. *Cold Spring Harb Perspect Biol*. 2011; 3:a004697.

- 478 **Simons K**, Toomre D. Lipid rafts and signal transduction. *Nature Rev Mol Cell Biol.* 2000; 1:31–39.
- 479 **Stone MB**, Shelby SA, Núñez MF, Wisser K, Veatch SL. Protein sorting by lipid phase-like domains supports  
480 emergent signaling function in B lymphocyte plasma membranes. *eLife.* 2017; 6:e19891.
- 481 **Stow JL**, Ching Low P, Offenhäuser C, Sangermani D. Cytokine secretion in macrophages and other cells:  
482 Pathways and mediators. *Immunobiology.* 2009; 214:601–612.
- 483 **Sung MH**, Li N, Lao Q, Gottschalk RA, Hager GL, Fraser IDC. Switching of the Relative Dominance Between  
484 Feedback Mechanisms in Lipopolysaccharide-Induced NF- $\kappa$ B Signaling. *Sci Signal.* 2014; 7:ra6–ra6.
- 485 **Tatano Y**, Shimizu T, Tomioka H. Unique Macrophages Different from M1/M2 Macrophages Inhibit T Cell  
486 Mitogenesis while Upregulating Th17 Polarization. *Sci Rep.* 2014; 4.
- 487 **Taylor PR**, Martinez-Pomares L, Stacey M, Lin HH, Brown GD, Gordon S. Macrophage Receptors and Immune  
488 Recognition. *Ann Rev Immunol.* 2005; 23:901–944.
- 489 **Tisza MJ**, Zhao W, Fuentes JSR, Prijic S, Chen X, Levental I, Chang JT. Motility and stem cell properties induced by  
490 the epithelial-mesenchymal transition require destabilization of lipid rafts. *Oncotarget.* 2016; 7:51553–51568.
- 491 **Tobias PS**, Soldau K, Ulevitch RJ. Isolation of a lipopolysaccharide-binding acute phase reactant from rabbit  
492 serum. *J Exp Med.* 1986; 164:777–793.
- 493 **Triantafilou M**, Brandenburg K, Kusumoto S, Fukase K, Mackie A, Seydel U, Triantafilou K. Combinational  
494 clustering of receptors following stimulation by bacterial products determines lipopolysaccharide responses.  
495 *Biochem J.* 2004; 381:527–536.
- 496 **Triantafilou M**, Miyake K, Golenbock DT, Triantafilou K. Mediators of innate immune recognition of bacteria  
497 concentrate in lipid rafts and facilitate lipopolysaccharide-induced cell activation. *J Cell Sci.* 2002; 115:2603–  
498 2611.
- 499 **Vasan M**, Wolfert MA, Boons GJ. Agonistic and antagonistic properties of a Rhizobium sin-1 lipid A modified by  
500 an ether-linked lipid. *Org Biomol Chem.* 2007; 5:2087–2097.
- 501 **Vats D**, Mukundan L, Odegaard JI, Zhang L, Smith KL, Morel CR, Greaves DR, Murray PJ, Chawla A. Oxidative  
502 metabolism and PGC-1 $\beta$  attenuate macrophage-mediated inflammation. *Cell Metabolism.* 2006; 4.
- 503 **Veatch SL**, Cicuta P. In: Bassereau P, Sens P, editors. *Critical Lipidomics: The Consequences of Lipid Miscibility in*  
504 *Biological Membranes* Cham, Switzerland: Springer; 2018. p. 141–168.
- 505 **Veatch SL**, Cicuta P, Sengupta P, Honerkamp-Smith A, Holowka D, Baird B. Critical Fluctuations in Plasma  
506 Membrane Vesicles. *ACS Chem Biol.* 2008; 3:287–293.
- 507 **Weinberger A**, Tsai FC, Koenderink GH, Schmidt TF, Itri R, Meier W, Schmatko T, Schröder A, Marques C. Gel-  
508 Assisted Formation of Giant Unilamellar Vesicles. *Biophys J.* 2013; 105:154–164.
- 509 **Wong SW**, Kwon MJ, Choi AMK, Kim HP, Nakahira K, Hwang DH. Fatty Acids Modulate Toll-like Receptor 4  
510 Activation through regulation of Receptor Dimerization and Recruitment into Lipid Rafts in a Reactive Oxygen  
511 Species-dependent Manner. *J Biol Chem.* 2009 Oct; 284:27384–27392.
- 512 **Wright SD**, Ramos RA, Tobias PS, Ulevitch RJ, Mathison JC. CD14, a receptor for complexes of lipopolysaccharide  
513 (LPS) and LPS binding protein. *Science.* 1990 Sep; 249:1431–1433.

Stimulation	$T_m$ (°C)	$T_m$ err (°C)	$\sigma$ (K)	$\sigma$ err (K)
IL4	14.54	1.06	5.46	1.56
	12.42	0.98	3.28	0.99
	12.42	0.79	3.19	0.81
	10.46	0.33	3.35	0.35
UNST	18.91	0.89	5.45	1.57
	14.56	0.80	5.75	1.24
	15.88	0.46	4.39	0.61
	18.18	0.43	4.17	0.56
	14.00	0.69	5.20	0.99
	13.11	0.49	4.90	0.62
	15.88	0.46	4.39	0.61
	16.44	0.83	4.28	1.03
	14.82	0.70	4.23	1.31
	14.21	1.02	5.31	1.44
	16.95	0.50	6.79	0.85
16.11	0.60	8.25	1.12	
IFN	20.38	0.99	6.79	1.97
	19.04	0.87	6.73	1.51
	18.81	0.45	5.09	0.78
LPS	20.15	0.20	3.84	0.30
	18.77	0.89	7.12	1.63
	18.36	0.61	4.84	1.03
	15.74	0.93	7.50	1.59
	21.33	0.41	4.95	0.72
	16.35	0.74	6.27	1.51
KLA	15.93	0.88	6.35	1.43
	25.93	0.90	6.02	1.68
	15.63	1.00	7.60	1.70
TLR4 <sup>-/-</sup> UNST	16.48	0.68	4.22	1.06
TLR4 <sup>-/-</sup> KLA	15.43	0.93	4.84	1.38

**Table 1.** Summary of the numerical values of the miscibility temperature and transition width obtained fitting the data with the empirical function  $f(T) = A [\tanh((T - T_m)/\sigma) + 1] + C$ .

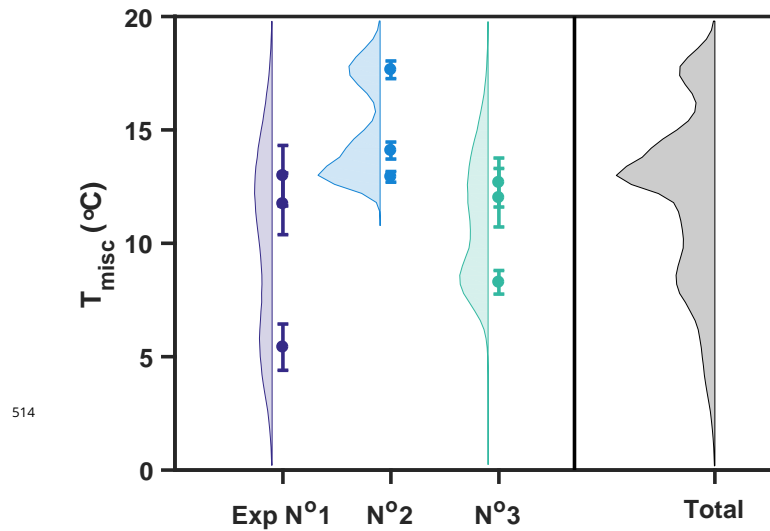


**Figure 4-Figure supplement 1.** Miscibility temperature of three repetitions of the same experiment in which macrophage cells at the same density are cultured in three separate flasks as replicates for two days. The data points have a wide temperature range both within the replicates and comparing the three experiments. Data points are also interpreted as representative of a whole distribution with the same average and standard deviation. In spite of the large variation, the sum of the distributions shows a main peak around 13°C. Continuous distributions are obtained simulating gaussian distributed numbers with mean and standard deviation equal to the value of the data and their error.

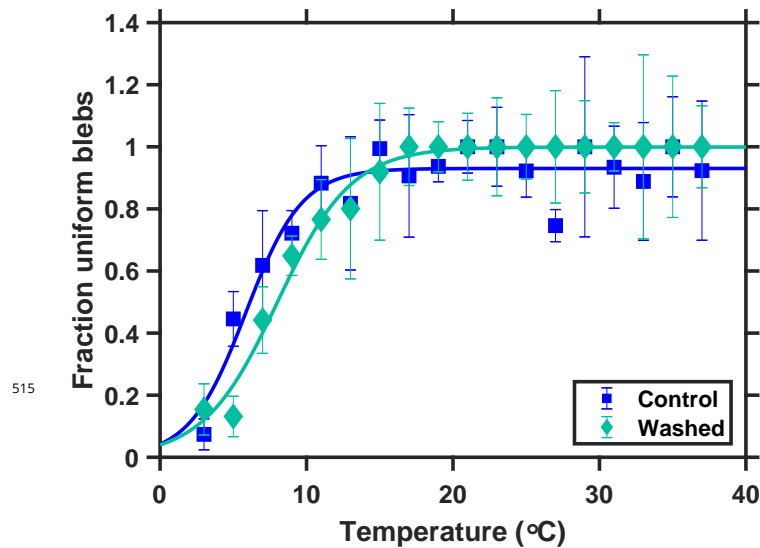


**Figure 4-Figure supplement 2.** Control experiment to test the effect of intracellular communication through secretion of cytokines on the melting temperature of GPMVS. The two samples were plated at the same density, and blebbing was induced after 12 hours during which the medium of the "washed" sample was changed every two hours. The control sample shows a lower  $T_m$  compared to the "washed", see Figure 4-supplement 2. This is compatible with a scenario in which the control condition is affected by an accumulation of M2-inducing cytokines like IL4.  $T_{control} = 5.8 \pm 1.0$ ,  $T_{washed} = 7.9 \pm 1.2$



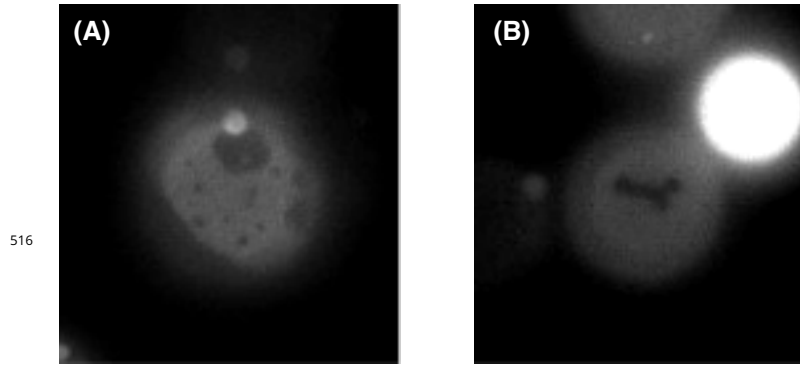


**Figure 5-Figure supplement 1.** Example GPMVs showing round domains (A) and an irregular domain (B). These different shapes likely correspond respectively to liquid-liquid and liquid-gel phase coexistence.

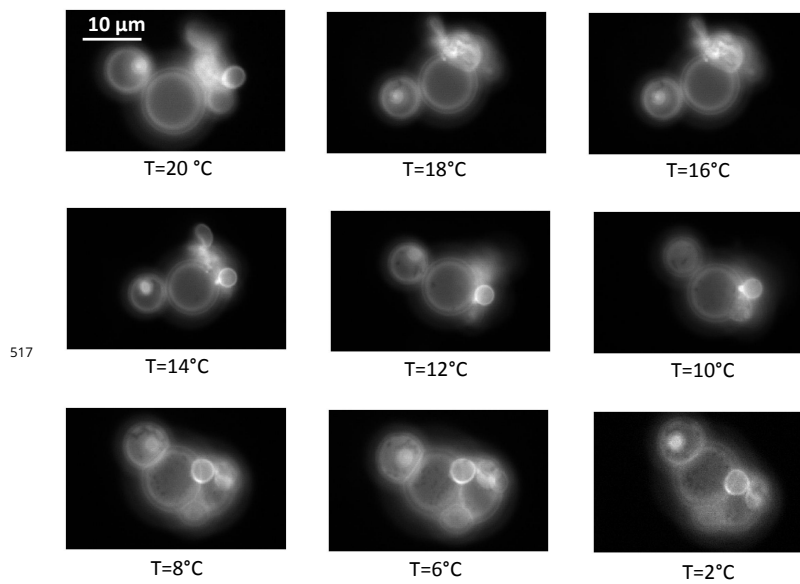


**Figure 6-Figure supplement 1.** In the same way as the 'parent' GPMV, it has been checked that vesicles reformed from just the lipid fraction purified from GPMVs undergo phase separation. The images show phase separation (dark domains) appearing at 18 and 12°C.